Chao Zhou[a], Xiangyi Feng[a], Zhangzhi Shi, Caixia Song, Xiaoshan Cui, Junwei Zhang, Ting Li, Egon Steen Toft, Junbo GE, Luning Wang* and Haijun Zhang*

Research on elastic recoil and restoration of vessel pulsatility of Zn-Cu biodegradable coronary stents

https://doi.org/10.1515/bmt-2019-0025
Received January 28, 2019; accepted June 24, 2019; online first September 17, 2019

Abstract: Coronary stents made of zinc (Zn)-0.8 copper (Cu) (in wt%) alloy were developed as biodegradable metal stents (Zn-Cu stents) in this study. The mechanical properties of the Zn-Cu stents and the possible gain effects were characterized by *in vitro* and *in vivo* experiments compared with 316L stainless steel stents (316L stents). Young's modulus of the as-extruded Zn-0.8Cu alloy and properties of the stents, including their intrinsic elastic recoil, stent trackability were evaluated compared with 316L stents. *In vivo* study was also conducted to evaluate restoration of pulsatility of vessel segment implanted stents. Both Zn-Cu stents and 316L stents have good acute lumen gain. By comparison, the advantages of Zn-Cu stents are as follows: (I) Zn-Cu stents have less intrinsic elastic recoil than 316L stents; (II) stent trackability indicates that Zn-Cu stents have a smaller push force when passing through curved blood vessels, which may cause less mechanical stimulation to blood vessels; (III) *in vivo* study suggests that Zn-Cu stents implantation better facilitates the recovery of vascular pulsatility.

Keywords: intrinsic elastic recoil; restoration of pulsatility; Young's modulus; zinc alloy stents.

[a]**Chao Zhou and Xiangyi Feng:** These authors contributed equally to this study.
***Corresponding authors: Luning Wang,** School of Materials Science and Engineering, University of Science and Technology Beijing, Beijing 100083, P.R. China; and **Haijun Zhang,** Department of Interventional and Vascular Surgery, The Tenth People's Hospital of Shanghai, Tongji University, Shanghai 200072, P.R. China; Branden Industrial Park, Qihe Economic and Development Zone, Dezhou City, Shandong 251100, P.R. China; and Department of Health Science and Technology, Faculty of Medicine, Aalborg University, Aalborg, Denmark, E-mail: luning.wang@ustb.edu.cn (L. Wang); zhanghaijun@tongji.edu.cn (H. Zhang)
Chao Zhou, Zhangzhi Shi and Ting Li: School of Materials Science and Engineering, University of Science and Technology Beijing, Beijing 100083, P.R. China
Xiangyi Feng, Caixia Song, Xiaoshan Cui and Junwei Zhang: National United Engineering Laboratory for Biomedical Material Modification, Branden Industrial Park, Qihe Economic and Development Zone, Dezhou City, Shandong 251100, P.R. China
Egon Steen Toft: Vice President for Medical and Health Sciences, Medical and Health Sciences Office, College of Medicine, Qatar University, Doha, Qatar
Junbo GE: Shanghai Institute of Cardiovascular Diseases, Zhongshan Hospital, Fudan University, 180 Fenglin Road, Shanghai 200032, P.R. China

Introduction

As early as in 2011, the European Medicines Agency approved the use of the Absorb Bioresorbable Vascular Scaffold (BVS) (Abbott Vascular, Santa Clara, CA, USA) made of a biodegradable poly-L-lactic acid (PLLA) polymer [1]. However, clinical data for the Absorb II [2], Absorb III [3], Absorb China [4], and Absorb Japan [5], showed that the composite endpoints of the target vessel, such as myocardial infarction in the Absorb stent had high values, leading to suggestions that the Absorb scaffold could not completely avoid the formation of late thrombosis, resulting in late lumen injuries, when compared to drug-eluting stents [6]. One possible explanation for this may be that the mechanical properties of polylactic acid materials are inferior to metal materials, and polylactic acid stents are thicker than the new generation of drug-eluting stents (BVS wall thickness is approximately 150 μm, while the thickness of the traditional metal stent is 80 μm) [7].

Biodegradable metal stents overcome the disadvantages of polylactic acid materials. In recent years, research on biodegradable zinc (Zn) alloy coronary stents have attracted increasing [8, 9]. Copper (Cu) is an essential trace element affecting the expression of specific genes and enzymes [10]. The Cu^{2+} promotes the secretion of endothelial nitric oxide synthase (eNOS), which helps maintain vascular endothelial integrity and endothelial cell function and stimulates the secretion of vascular endothelial growth factor (VEGF) [11, 12]. Rapid reendothelialization of blood vessels occurs at the site of stent implantation, and promotes angiogenesis at the site of myocardial infarction

[13]. In order to avoid the influence of the excessive and uneven distribution of the second phase to corrosion [14], Zn-0.8Cu alloys were made into Zn-Cu coronary stents in this research.

Schmidt et al. [15] studied the mechanical properties of current biodegradable stents including biodegradable magnesium alloy stents [Magmaris (BIOTRONIK AG, Bülach, Switzerland)] and PLLA stents [Absorb GT1 (Abbott Vascular, Temecula, CA, USA) and DESolve (Elixir Medical Corporation, Sunnyvale, CA, USA)]. Biodegradable metal stents overcome some of the shortcomings of polymer stents, but there is still little data on the mechanical properties compared to permanent metal stents of identical structure. As a coronary stent, in addition to the biodegradability, the mechanical properties of the stent are also valued in order to provide more evidence in clinical comparative studies. The mechanical properties of Zn-Cu stents were characterized in this study compared to 316L stents. Zn-0.8Cu is made into a coronary stent with a size of 3.0 mm in diameter and 20 mm in length in an expanded state (the following abbreviated as ϕ3.0 mm×20 mm) by the Rientech Med Tec Co., Ltd. (Qihe, China). The elastic intrinsic recoil and trackability of stents were studied *in vitro*. We also investigated the lumen gain and recovery of blood vessel elasticity in porcine coronary arteries, implanted with Zn-Cu stents and 316L stainless steel stents.

Materials and methods

Zn-Cu alloy preparation

Binary Zn-0.8Cu (in wt%) alloy ingots were fabricated using pure Zn (99.995 wt%) (Hulu Dao Zinc Industry Co., Ltd., China) and pure Cu (99.995 wt%) (ZhongNuo Advanced Material (Beijing) Technology Co., Ltd., Beijing, China). Melting was performed in a graphite resistor furnace under air atmosphere at 650–680°C. Then, it was cooled into an ingot of 100 mm in diameter and 400 mm in length. The ingot was made into a coronary stent by drawing and laser cutting.

Stents processing

The permanent metal stents (316L stents) were made of 316L stainless steel (316L SS). The zinc-alloy metal stents (Zn-Cu stents) were made of Zn-0.8Cu alloy. The stents used for the test in this study were balloon-expandable stents. All stents were 3 mm in outer diameter and 20 mm in length when they were expanded at 8 standard atmospheric pressure (atm) and the structural thickness was 0.127 mm. The stent structure is shown in Figure 1. Both Zn-Cu stents and 316L stents have the same structure.

The 316L stents were commercialized drug-eluting stents received from Rientech Med Tec Co., Ltd. (Qihe, China) with the trade name Cordimax™ since 2012 in China [16]. Zn-Cu stents were also made by Rientech Med Tec Co., Ltd. (Qihe, China). Stents for implantation (both Zn-Cu stents group and 316L stents group) were spray-coated with the polymer/sirolimus coating matrix using a MediCoat YM II Stent Coating System (Sono-Tek Corp., Milton, NY, USA). The polymer used was poly (D, L-lactide-co-glycolide) (PLGA, LA:GA = 70:30) [17, 18].

Intrinsic elastic recoil and trackability

Both intrinsic elastic recoil and stent trackability are critical determinants of the mechanical properties of coronary stents. Low intrinsic elastic recoil helps reduce immediate lumen loss. The trackability describes the ability of a stent system to be advanced through a curved vessel. These two properties have a great influence on the use of the stent in clinical settings. The experimental details are as follows:

Intrinsic elastic recoil of balloon-expandable stents: the intrinsic elastic recoil of stents refers to the reduction in diameter of the stent when the balloon is deflated from a nominal pressure to zero which is shown as a schematic diagram in Figure 2. According to ASTM F 2079-2013 [19], measurements were made at multiple axial locations, including one location near the midlength and locations near either end of the stent. To allow for full expansion of the stent, the expansion pressure needs to be maintained for 15 s–30 s before taking the diameter measurements. The test was performed by a precision image measuring instrument (VMS-1510G, purchased from Beijing Huilong Technology Co., Ltd., China). The intrinsic elastic recoil rate was calculated by equation (1):

$$\text{Elastic intrinsic recoil}\ (\%) = \left(1 - \frac{D_{\text{final}}}{D_{\text{inflated}}}\right) \times 100 \quad (1)$$

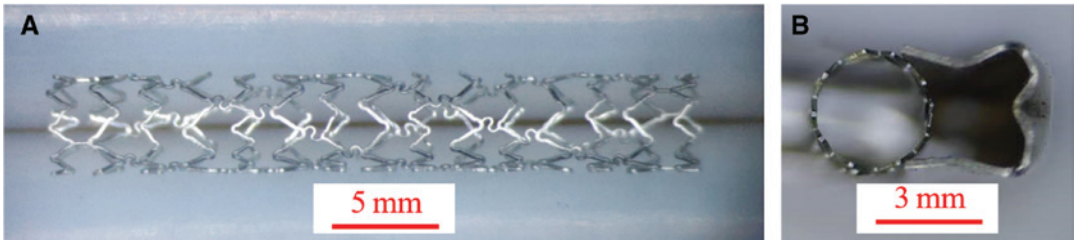

Figure 1: Physical structure of the expanded stent.
(A) Main view, (B) top view.

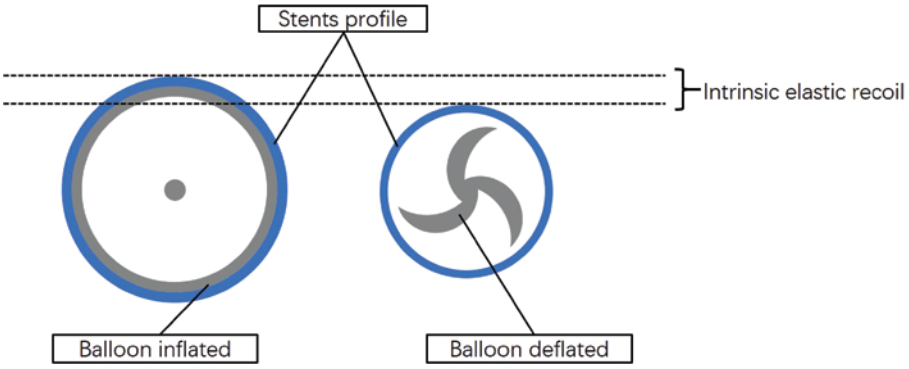

Figure 2: Schematic diagram of intrinsic elastic recoil.

where $D_{inflated}$, outer diameter of stent while on an inflated delivery balloon; D_{final}, outer diameter of stent after deflating the delivery balloon.

Trackability: coronary vessels were simulated with an alternative test tracking fixture [20] as shown in Figure 3. The balloon-expandable stent system was pushed through the alternative test tracking fixture and the push forces required were measured. An alternative test tracking fixture was made of acrylic materials with reference to ASTM F2394-07 (2017) [20]. The longest path (A→B→C→D→E→F) was chosen to test the stent trackability. There was no need to manually adjust the direction of stent's movement when passing through this path, thereby avoiding manual error to the force sensor. The maximum push force was recorded to compare the trackability between the two stents. Three samples of different stents were tested. The smaller the push force the stents required, the better the trackability the stents had.

Radial strength and bending force

In order to better and more comprehensively describe the mechanical properties of the stent, the radial strength and bending force test were supplemented.

Radial strength: The Radial strength test used a radial strength tester (TTE2, Blockwise, USA). Zn-Cu stents and 316L stents were firstly inflated to the nominal diameter (3.0 mm) and released under human body temperature. The values of radial strength vs. compressive diameter were recorded by the computer at a compression rate of 0.1 mm/s. The radial strength (kPa) of the stents was defined as the strength at 10% compression of the initial compression diameter.

Bending force: the bending force was evaluated by using a three-point bend test. Two parallel rods 8 mm in diameter separated by 16 mm center-to-center. The rods formed the endpoints of the three-point bend test. A hook claimed by the universal testing machine CMT4105 (MTSSANS Co., Ltd., Shenzhen, China) provided vertical traction to the midpoint of the unexpanded stent without a delivery system (Figure 4). The bending force can simply characterize the flexibility of stents. The smaller bending force the stents had, the better flexibility the stents had.

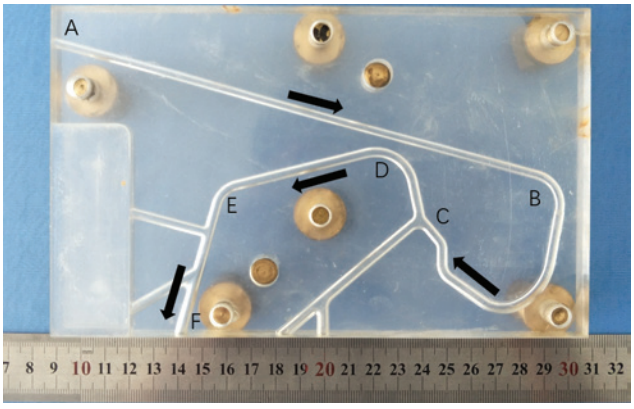

Figure 3: The alternative test tracking fixture.

Young's modulus of the as-extruded Zn-0.8Cu alloy

The size of all stents in this study was ϕ3.0 mm×20 mm, so the Young's modulus of the as-extruded Zn-0.8Cu alloy with 3 mm in diameter was tested. The Young's modulus of tensile specimen was determined using the dynamic method. The mechanical resonance frequency of the sample was determined by the elasticity modulus, density and size of the material. Therefore, the elastic modulus of the material can be determined by the geometry size of the sample, the density and the mechanical resonance frequency of determined mode and level. Young's modulus was calculated by equation (2):

$$E = 1.6067 \times 10^{-9} \left(\frac{l}{d}\right)^3 \frac{m}{d} f_1^2 T_1 \quad (2)$$

where E, dynamic Young's modulus (GPa); l, length of sample (mm); d, outer diameter of sample (mm); m, quality of sample (g); f_1, the mean resonance frequency of sample under fundamental frequency (Hz); T_1, correction factor when the sample vibration under fundamental frequency.

Tensile mechanical properties of the as-extruded Zn-Cu alloy

The expansion of stents includes plastic deformation, so the mechanical properties of the stents are also related to the mechanical

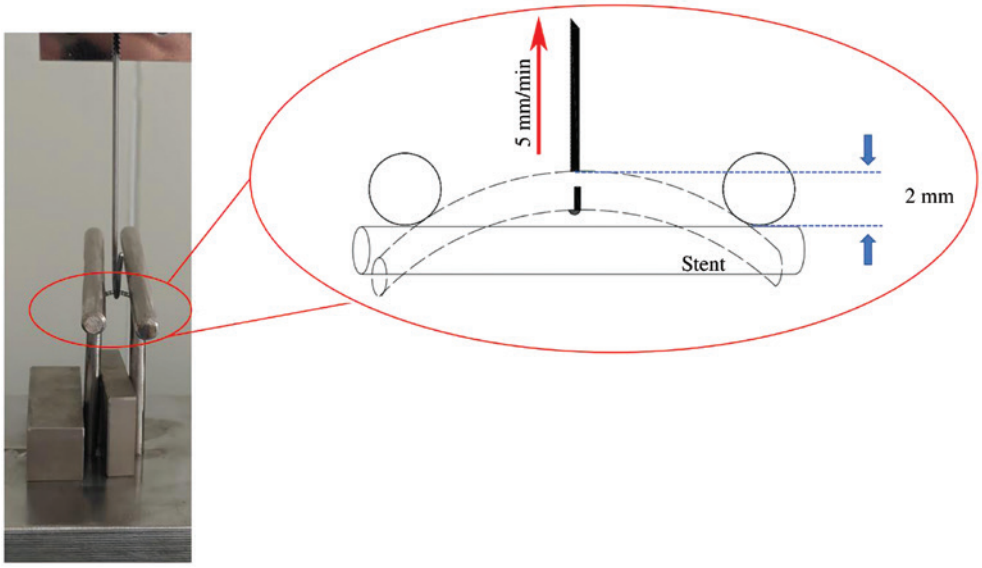

Figure 4: Schematic diagram of bending force.

strength of the materials. The size of all stents in this study was ϕ3.0 mm × 20 mm, so the tensile properties of the as-extruded Zn-0.8Cu alloy with 3 mm in diameter was characterized. The specimen was 140 mm in parallel length and 100 mm in original gauge length. Tensile mechanical tests were performed on a universal testing machine CMT4105 (MTSSANS Co., Ltd., Shenzhen, China) referring to standard ASTM-E8-04 [21]. The as-extruded materials were tested at a strain rate of 2.5×10^{-4} s^{-1} (15 mm/min) at room temperature (22°C).

Acute lumen loss and restoration of pulsatility

Both Zn-Cu stents and 316L stents were implanted into porcine coronary arteries in two different pigs. Stents were implanted in three coronary arteries in each pig including the right coronary artery (RCA), the left circumflex artery (LCX) and the left anterior descending artery (LAD). The pigs were female Shanghai White pig models (purchased from Shanghai Jiagan Biotechnology Co., Ltd., 6-month old, weighing 40–50 kg). Blood pressure was monitored throughout the procedure in real time. Animal experiments were approved by the Animal Ethics Committee of Zhongshan Hospital (Shanghai, China), and carried out under the National Institutes of Health Guide for Care and Use of Laboratory Animals.

Acute lumen loss: quantitative coronary angiography (QCA) measured the difference of diameter in the blood flow channel when the balloon was inflated and deflated. The diameter of the reference vessel, instant and post-implantation on the target vessel were measured using an internal digital calipers of the fluoroscope with the guiding catheter serving as a reference for calibration (QCA, using the GE Innovia 2000 IQ system, USA). The basic principles of the video-densitometric technique have been described previously [22]. This technique is based on the relationship between the attenuating power of the lumen filled with contrast medium and the X-ray image intensifier. The diameter is measured by using edge-detection techniques [23]. The reference vessel and the stent-implanted vessel are 5 mm apart and both are 20 mm long.

Restoration of pulsatility: at the designated experimental endpoint (18 months), the pigs were anesthetized and stent-implanted arteries were assessed by intravascular ultrasound (IVUS) images (iLab Ultrasound Imaging System, 40-Mz catheter, Boston Scientific, Natick, MA, USA), which captured mid regions of stented segments. Pulsating blood vessels from the end of systole to the end of diastolic blood vessels were recorded by the IVUS manual mode at fixed points. Similarly, 15 still frame images in each blood vessel were collected at the end of systole and diastole cycles. The lumen area (LA) was measured in each frame. The pigs were humanely euthanized after IVUS imaging. The value of ΔLA can reflect the pulse recovery of blood vessels and the stent's trackability.

Results

Mechanical properties of stents and materials

The mechanical properties of Zn-Cu stents and 316L stents *in vitro* are summarized in Table 1.

The maximum push force of the 316L stents is 1.73 N, higher than that of Zn-Cu stents (1.21 N). The less push

Table 1: The mechanical test of Zn-Cu stents and 316L stents *in vitro*.

Stent	Maximum push force (N)	Intrinsic elastic recoil (%)	Bending force (N)	Radial strength (kPa)
Zn-Cu	1.21 ± 0.09	0.41 ± 0.18	0.14 ± 0.02	112.60 ± 3.18
316L	1.73 ± 0.11	1.84 ± 0.61	0.54 ± 0.12	185.84 ± 13.19

force the stent needs, the better trackability the stent has. This indicates that Zn-Cu stents move easily through a curved vascular pathway, and lower push force also can reduce damage to the vessel wall during the delivery. The intrinsic elastic recoil rate of Zn-Cu stents is 0.41% and that of 316L stents is 1.84%. This suggests Zn-Cu stents may cause less acute lumen loss compared to the 316L stents, which is beneficial for the establishment of blood flow channels. The bending force of the unexpanded stents was 0.14 ± 0.02 N and 0.54 ± 0.12 N for the two different stents, Zn-Cu stents and 316L stents, respectively. Zn-Cu stents may follow the curved vessel contour better than 316L stents. The radial strength of Zn-Cu stents is lower than 316L stents. The radial strength of Zn-Cu stents is 112.6 kPa which is lower than 185.84 kPa of 316 stents.

The tensile properties and Young's modulus of the as-extruded Zn-Cu alloy and 316L stainless steel are summarized in Table 2. Young's modulus of Zn-Cu materials is less than half of 316L stainless steel. The yield strength (YS) and ultimate tensile strength (UTS) of 316L stainless steel are much higher than that of the as-extruded Zn-Cu alloy in this study. The YS and UTS of as-extruded Zn-Cu alloy in this study are 110.0 ± 4.9 MPa and 142.7 ± 9.2 MPa, respectively. YS and UTS of 316L stainless steel are 252 MPa and 550 MPa, respectively. But the elongation of the as-extruded Zn-Cu alloy is 193.8 ± 2.5% which is higher than 72% [24] of 316L stainless steel.

Acute lumen loss and restoration of pulsatility

Figure 5 shows representative QCA still frames of Zn-Cu stents- and 316L stents in implanted porcine coronary arteries. It can be seen that both stents are successfully inflated in the blood vessels. The acute lumen loss about Zn-Cu stents and 316L stents implanted in porcine coronary arteries is shown in Table 3. The acute lumen loss of Zn-Cu stents is similar to 316L stents (4.40 ± 3.75% vs. 5.11 ± 1.56%, $p = 0.78$). The difference between the values is not statistically significant ($p > 0.05$).

Figure 6(A) and (B) show lumen areas (LAs) captured in the mid-implanted area of Zn-Cu stents- and 316L stents-implanted arteries in end-diastole and both Zn-Cu stent and 316L stent did not cause significant in-stent restenosis. The differences in diameter of the red circle and the yellow circle represent the thickness of the tunica intima. Both Zn-Cu stents and 316L stents are covered by endothelial cells. The tunica intima thickness of vessel that Zn-Cu stent and 316L stent implanted are both 0.5 mm on average. The LAs were captured in the mid-implanted areas of Zn-Cu stents- and 316L stents-implanted arteries at the same position, in end-diastolic and end-systolic states. This is to examine changes in pulsatility of stent implanted vessel segments over time. The results show a return of pulsatility in Zn-Cu stents-implanted arteries, as indicated by the absolute difference in lumen cross-sectional areas, observed from systole to diastole (ΔLA).

Table 2: The mechanical properties of as-extruded Zn-0.8Cu alloy and 316L SS.

	Yield strength (MPa)	Ultimate tensile strength (MPa)	Elongation (%)	Young's modulus (GPa)
Zn-0.8Cu	111.0 ± 4.9	142.7 ± 9.2	193.8 ± 2.5	89.10 ± 6.26
316L Stainless steel [24]	252	550	75	200

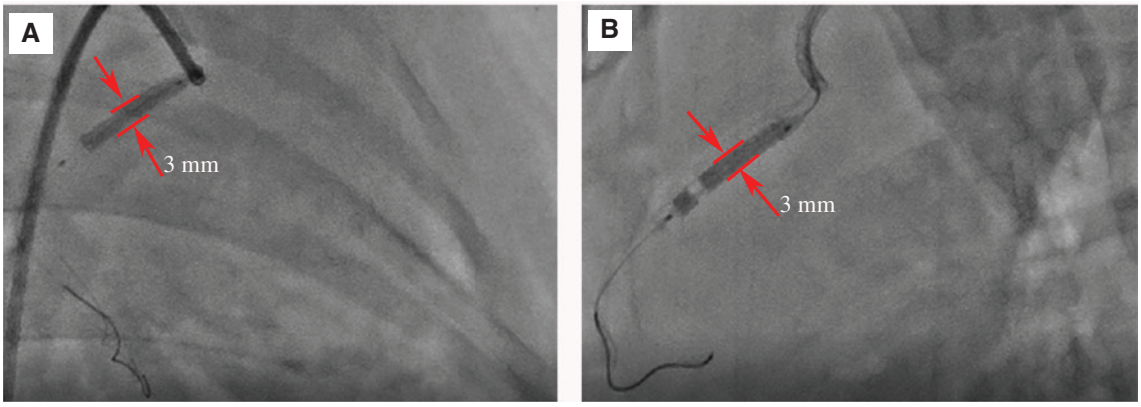

Figure 5: Representative QCA still frames of Zn-Cu stents- and 316L stents-implanted porcine coronary arteries when the balloon is inflated. (A) Zn-Cu stents-implanted in RCA; (B) 316L stents-implanted in RCA.

Table 3: The measurements of acute lumen loss.

Group	Reference vessel diameter (mm)	Instant vessel diameter (mm)	Instant diameter after implantation (mm)	Acute lumen loss
Zn-Cu group	2.79 ± 0.37	2.94 ± 0.16	2.81 ± 0.18	4.40 ± 3.75%
316L Stainless steel group	2.84 ± 0.27	2.82 ± 0.21	2.74 ± 0.28	5.11 ± 1.56%
p-Value	0.63	0.81	0.76	0.78

Figure 6C depicts the average ΔLA for stent implanted segments at 18 months. At 18 months, the mean ΔLAs of Zn-Cu stents in three different vessels are 1.12 mm^2, 0.73 mm^2 and 0.78 mm^2, respectively. The mean ΔLAs of 316L stents in three different vessels are 0.18 mm^2, 0.15 mm^2 and 0.20 mm^2, respectively. The difference between the values is statistically significant ($p < 0.05$). The ΔLA of Zn-Cu stents-implanted arteries was generally higher than that of 316L stents-implanted, indicating an improved restoration of pulsatility of blood vessels for Zn-Cu stent. The larger the ΔLA value, the better pulsatility the blood vessels recover.

Discussion

When the delivery system is identical, the performance of the stent is mainly related to the material and structure. The two types of stents tested in this study are identical in structure. Therefore, the main factor affecting the properties

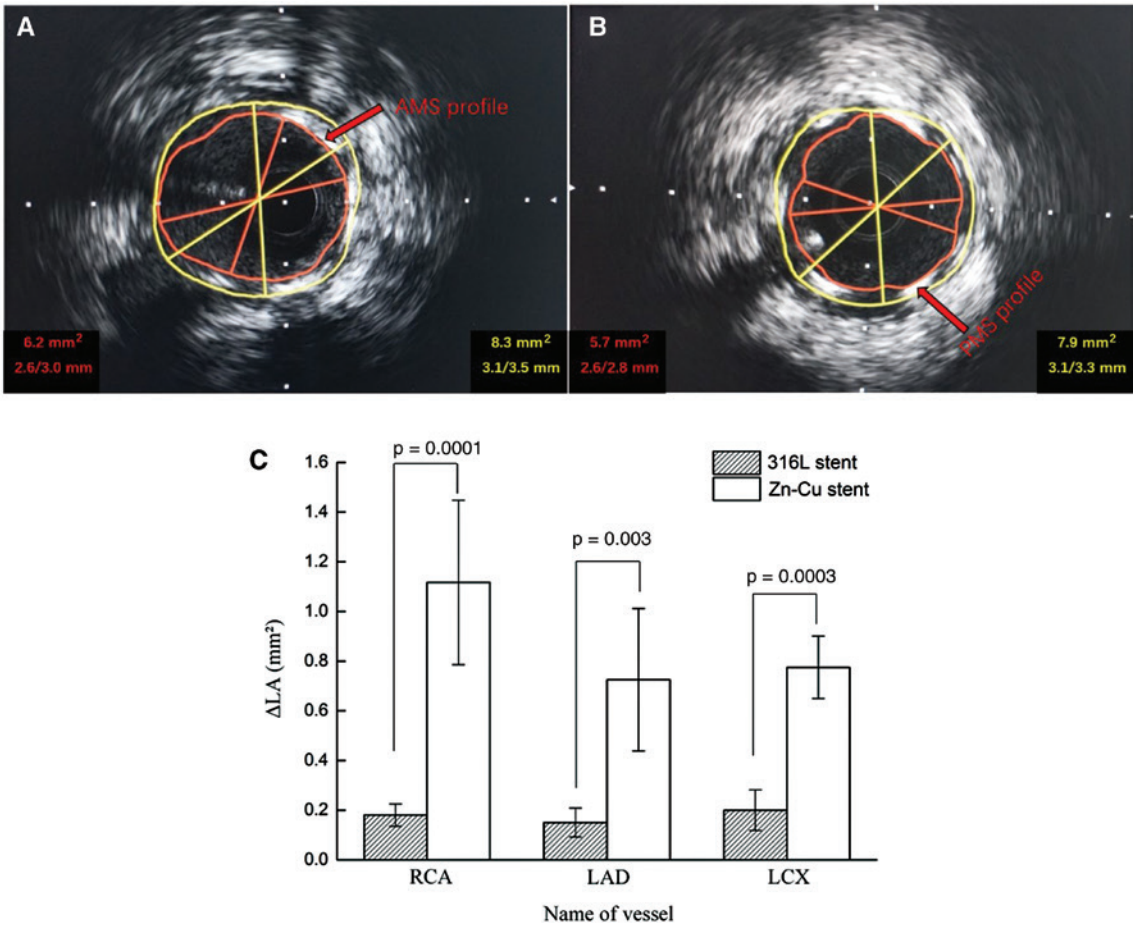

Figure 6: Representative photomicrographs of IVUS in porcine right coronary arteries.
(A) Zn-Cu stent and (B) 316L stent (C) ΔLA for Zn-Cu stent- and 316L stent-implanted porcine coronary arteries after 18 months. The differences in diameter of the red circle and the yellow circle represent the thickness of the tunica intima.

of stents is the difference in material properties between Zn-0.8Cu and 316L stainless steel. The stent expansion process includes balloon inflation and deflation. The former causes a large plastic deformation of the stent, which is related to the plasticity of the material. And the stent will recoil after balloon deflation which is related to intrinsic elastic performance of materials. In this study, Young's modulus is used to characterize the elastic properties of the material.

The less intrinsic elastic recoil is beneficial for lumen gain in clinical [15]. The as-extruded Zn-0.8Cu alloy exhibits lower Young's modulus than that of 316L stainless steel which indicates the 316L stents' ability to resist balloon expansion is much higher than Zn-Cu stents. In this study, the as-extruded Zn-0.8Cu alloy exhibits superplasticity at room temperature according to the elongation of 193.8%, which suggests Zn-Cu stents have an excellent plastic deformation when they are inflated. And in recent studies about room temperature superplasticity of zinc alloy, Bednarczyk et al. [25] found the room temperature superplasticity of Zn-0.5Cu by equal channel angular pressing. And Mostaed et al. [26] also reported the strain induced precipitates a drastic drop in the tensile strength and promotes strain rate sensitivity due to the activation of $Zn/CuZn_4$ boundary sliding. This is another reason for lower recoil of the Zn-Cu stent. Schmidt et al. [15] have studied the recoil of Magmaris stents (Biotronic), the results show that the recoil of Magmaris is about 5.0%. But the stent system and measurement methods are different, the difference of results cannot be explained by the material properties only.

The trackability is a critical performance when they are used in some complex lesions. When the stent system passes through the blood vessel, the stent bending process mainly occurs. And the trackability is also related to Young's modulus of materials [27]. The YS and UTS of the as-extruded Zn-Cu alloy in this study are lower than that of 316L stainless steel. These lower mechanical strength of Zn-Cu materials causes lower radial strength. But on the other hand, Zn-Cu stents have a lower bending force which may make the long stents exhibit good flexibility in the blood vessels.

The structure of the vessel wall includes the intima, media and adventitia. Endothelialization occurs after stent implantation [28, 29]. The IVUS images demonstrated the proliferation of the tunica intima. The finding that Young's modulus of the intima-media layer of the pig's thoracic aorta is just 43.2 ± 15.8 kPa in the small stress, small strain regime [30]. Normal coronary arteries were exposed to shear stress and cyclic strain [31, 32]. The mechanical stress and strain affect the anatomy and function of endothelial cells and smooth muscle cells and regulate vascular remodeling [33–35]. Previous animal studies by Schwartz et al. [36, 37] and Karas et al. [38] established a significant correlation between the degree of arterial injury caused by metallic wire coils and the resultant neointimal thickness and lumen stenosis at the stented site. So, if the Young's modulus of the implanted materials is too large, it will cause stress mismatch and arterial injury. Upon 316L stents stenting, aberrant forces and disruption of normal vascular physiology have been reported, including adverse clinical events, such as stent thrombosis, neo-atherosclerosis and restenosis [39]. Zn-Cu stents can adapt to normal cyclic stress from end-systole to end-diastole in arteries.

The porcine coronary artery model is the preferred model for evaluating stent performance *in vivo*. In addition, the pigs used in this study were in the growth stage, their coronary arteries were different from diseased coronary arteries [40]. Differences between animal models may be responsible for the reduced variability in acute lumen loss. And for the restoration of pulsatility, it was not only related to the lesser stimulation of blood vessels by Zn-Cu stents, but also related to the degradation characteristics of Zn-Cu stents. The degradation characteristics of Zn-Cu stents will be reported in another study.

Conclusion

The mechanical properties of Zn-Cu novel coronary stents have been characterized compared with 316L stents. The Young's modulus of the stent's material affects the elastic recoil of the stent. Zn-Cu stents have less intrinsic elastic recoil and better trackability than that of 316L stents, all of which are crucial for coronary stenting applications. The acute lumen loss of Zn-Cu stents is a little lower than that of 316L stents. Compared with 316L stents, Zn-Cu stents may reduce side effects on vascular pulsation, and are conducive to restoring blood vessel elasticity.

Acknowledgements: Thanks for the technical support provided by Rientech Med Tec Co., Ltd. (Qihe Economic & Development Zone, 251100 Qihe, Shandong Province, China) regarding the preparation of the stent and the preparation of the stent production.

Author Statement

Research funding: This study has financial support from the National Key Research and Development Program of China (No. 2016YFC1102500).

Conflict of interest: Authors declare that there is no conflict of interest regarding the publication of this scientific article.

Informed consent: Informed consent is not applicable.

Ethical approval: This article does not contain any studies with human participants or animals performed by any of the authors.

References

[1] Iqbal J, Gunn J, Serruys PW. Coronary stents: historical development, current status and future directions. Br Med Bull 2013;106:193–211.

[2] Serruys PW, Chevalier B, Sotomi Y, Cequier A, Carrié D, Piek JJ, et al. Comparison of an everolimus-eluting bioresorbable scaffold with an everolimus-eluting metallic stent for the treatment of coronary artery stenosis (ABSORB II): a 3 year, randomised, controlled, single-blind, multicentre clinical trial. Lancet 2016;388:2479–91.

[3] Kereiakes DJ, Ellis SG, Metzger C, Caputo RP, Rizik DG, Teirstein PS, et al. 3-year clinical outcomes with everolimus-eluting bioresorbable coronary scaffolds: the ABSORB III trial. J Am Coll Cardiol 2017;70:2852–62.

[4] Gao R, Yang Y, Han Y, Huo Y, Chen J, Yu B, et al. Bioresorbable vascular scaffolds versus metallic stents in patients with coronary artery disease: ABSORB china trial. J Am Coll Cardiol 2015;66:2298–309.

[5] Kimura T, Kozuma K, Tanabe K, Nakamura S, Yamane M, Muramatsu T, et al. A randomized trial evaluating everolimus-eluting Absorb bioresorbable scaffolds vs. everolimus-eluting metallic stents in patients with coronary artery disease: Absorb Japan. Eur Heart J 2015;36:3332–42.

[6] Cassese S, Byrne RA, Ndrepepa G, Kufner S, Wiebe J, Repp J, et al. Everolimus-eluting bioresorbable vascular scaffolds versus everolimus-eluting metallic stents: a meta-analysis of randomised controlled trials. Lancet 2015;387:537–44.

[7] Im SH, Jung Y, Kim SH. Current status and future direction of biodegradable metallic and polymeric vascular scaffolds for next-generation stents. Acta Biomater 2017;60:3–22.

[8] Wang C, Yu Z, Cui Y, Zhang Y, Yu S, Qu G, et al. Processing of a novel Zn alloy micro-tube for biodegradable vascular stent application. J Mater Sci Technol 2016;32:925–9.

[9] Niu J, Tang Z, Huang H, Pei J, Zhang H, Yuan G, et al. Research on a Zn-Cu alloy as a biodegradable material for potential vascular stents application. Mater Sci Eng C 2016;69:407–13.

[10] Luza SC, Speisky HC. Liver copper storage and transport during development: implications for cytotoxicity. Am J Clin Nutr 1996;63:812S–20S.

[11] Sen CK, Khanna S, Venojarvi M, Trikha P, Ellison EC, Hunt TK, et al. Copper-induced vascular endothelial growth factor expression and wound healing. Am J Physiol Hear Circ Physiol 2002;282:H1821–7.

[12] Jiang Y, Reynolds C, Xiao C, Feng W, Zhou Z, Rodriguez W, et al. Dietary copper supplementation reverses hypertrophic cardiomyopathy induced by chronic pressure overload in mice. J Exp Med 2007;204:657–66.

[13] Mcauslan BR, Reilly W. Endothelial cell phagokinesis in response to specific metal ions. Exp Cell Res 1980;130:147–57.

[14] Gao JH, Guan SK, Ren ZW, Sun YF, Zhu SJ, Wang B. Homogeneous corrosion of high pressure torsion treated Mg-Zn-Ca alloy in simulated body fluid. Mater Lett 2011;65:691–3.

[15] Schmidt W, Behrens P, Brandt-Wunderlich C, Siewert S, Grabow N, Schmitz KP. *In vitro* performance investigation of bioresorbable scaffolds – standard tests for vascular stents and beyond. Cardiovasc Revasc Med 2016;17:375–83.

[16] Zhang H, Wang X, Deng W, Wang S, Ge J, Toft E. Randomized clinical trial comparing abluminal biodegradable polymer sirolimus-eluting stents with durable polymer sirolimus-eluting stents. Medicine 2016;95:e4820.

[17] Zhang H, Deng W, Wang X, Wang S, Ge J, Toft E. Solely abluminal drug release from coronary stents could possibly improve reendothelialization. Catheter Cardiovasc Interv 2016;88:E59–66.

[18] Zhang H, Li X, Deng W, Wang X, Wang S, Ge J, et al. Drug release kinetics from a drug-eluting stent with asymmetrical coat. Front Biosci 2017;22:407–15.

[19] ASTM F2079-09 (2017), Standard Test Method for Measuring Intrinsic Elastic Recoil of Balloon-Expandable Stents, ASTM International, West Conshohocken, PA, USA, 2017.

[20] ASTM F2394-07 (2017), Standard Guide for Measuring Securement of Balloon Expandable Vascular Stent Mounted on Delivery System, ASTM International, West Conshohocken, PA, USA, 2017.

[21] American Society for Testing and Materials, 2004a. ASTM-E8-04: standard test methods for tension testing of metallic materials. American society for testing and materials. In: annual book of ASTM standards. Philadelphia, PA: American Society for Testing and Materials.

[22] Serruys PW, Reiber JHC, Wijns W, van de Brand M, Kooijman CJ, ten Katen HJ, et al. Assessment of percutaneous transluminal coronary angioplasty by quantitative coronary angiography: Diameter versus densitometric area measurements. Am J Cardiol 1984;54:482–8.

[23] Zhang YJ, Bourantas CV, Muramatsu T, Iqbal J, Farooq V, Diletti R, et al. Comparison of acute gain and late lumen loss after PCI with bioresorbable vascular scaffolds versus everolimus-eluting stents: an exploratory observational study prior to a randomised trial. EuroIntervention 2014;10:672–80.

[24] Ren Y, Yang K, Zhang B, Wang Y, Liang Y. Nickel-free stainless steel for medical applications. J Mater Sci Technol 2004;20:571–3.

[25] Bednarczyk W, Kawałko J, Wątroba M, Bała P. Achieving room temperature superplasticity in the Zn-0.5Cu alloy processed via equal channel angular pressing. Mater Sci Eng A 2018;723:126–33.

[26] Mostaed E, Ardakani MS, Sikora-Jasinska M, Drelich JW. Precipitation induced room temperature superplasticity in Zn-Cu alloys. Mater Lett 2019;244:203–6.

[27] Schmidt W, Lanzer P, Behrens P, Topoleski LDT, Schmitz KP. A comparison of the mechanical performance characteristics of seven drug-eluting stent systems. Catheter Cardiovasc Interv 2009;73:350–60.

[28] Kim TH, Kim JS, Kim BK, Ko YG, Choi D, Jang Y, et al. Long-term (≥2 years) follow-up optical coherence tomographic study after sirolimus- and paclitaxel-eluting stent implantation: comparison to 9-month follow-up results. Int J Cardiovasc Imaging 2011;27:875–81.

[29] Babapulle MN, Joseph L, Bélisle P, Brophy JM, Eisenberg MJ. A hierarchical bayesian meta-analysis of randomised clinical trials of drug-eluting stents. ACC Curr J Rev 2004;13:55.
[30] Yu Q, Zhou J, Fung YC. Neutral axis location in bending and Young's modulus of different layers of arterial wall. Am J Physiol 1993;265:H52–60.
[31] Zhao S, Suciu A, Ziegler T, Moore JE Jr, Bürki E, Meister JJ, et al. Synergistic effects of fluid shear stress and cyclic circumferential stretch on vascular endothelial cell morphology and cytoskeleton. Arterioscler Thromb Vasc Biol 1995;15:1781–6.
[32] Chien S. Mechanotransduction and endothelial cell homeostasis: the wisdom of the cell. Am J Physiol Hear Circ Physiol 2007;292:H1209–24.
[33] Davies PF. Hemodynamic shear stress and the endothelium in cardiovascular pathophysiology. Nat Clin Pract Cardiovasc Med 2009;6:16–26.
[34] Gupta V, Grande-Allen KJ. Effects of static and cyclic loading in regulating extracellular matrix synthesis by cardiovascular cells. Cardiovasc Res 2006;72:375–83.
[35] Pasterkamp G, De Kleijn DP, Borst C. Arterial remodeling in atherosclerosis, restenosis and after alteration of blood flow: potential mechanisms and clinical implications. Cardiovasc Res 2000;45:843–52.
[36] Schwartz RS, Murphy JG, Edwards WD, Camrud AR, Vliestra RE, Holmes DR. Restenosis after balloon angioplasty. A practical proliferative model in porcine coronary arteries. Circulation 1990;82:2190–200.
[37] Schwartz RS, Huber KC, Murphy JG, Edwards WD, Camrud AR, Vlietstra RE, et al. Restenosis and the proportional neointimal response to coronary artery injury: results in a porcine model. J Am Coll Cardiol 1992;19:267–74.
[38] Karas SP, Gravanis MB, Santoian EC, Robinson KA, Anderberg KA. Coronary intimal proliferation after balloon injury and stenting in swine: an animal model of restenosis. J Am Coll Cardiol 1992;20:467–74.
[39] Lane JP, Perkins LEL, Sheehy AJ, Pacheco EJ, Frie MP, Lambert BJ, et al. Lumen gain and restoration of pulsatility after implantation of a bioresorbable vascular scaffold in porcine coronary arteries. JACC Cardiovasc Interv 2014;7:688–95.
[40] Mintz GS, Popma JJ, Pichard AD, Kent KM, Satler LF, Wong SC, et al. Arterial remodeling after coronary angioplasty a serial intravascular ultrasound study. Circulation 1996;94:35–43.